AIAA SciTech
13-17 January 2014, National Harbor, Maryland
10th AIAA Multidisciplinary Design Optimization Conference

Extensibility of a Linear Rapid Robust Design Methodology

Bradley A. Steinfeldt* and Robert D. Braun†
Georgia Institute of Technology, Atlanta, GA 30332-0150

This work examines the extensibility of a linear rapid robust design methodology enabled by viewing the multidisciplinary design optimization problem as a dynamical system to nonlinear problems. This analysis is approached from a computational and accuracy perspectives. The sensitivity of the solution's computational cost is examined by analyzing effects such as the number of design variables, nonlinearity of the CAs, and nonlinearity in addition to several potential complexity metrics. Relative to traditional robust design methods, the linear rapid robust design methodology scaled better with the size of the problem and had performance that exceeded the traditional techniques examined. The accuracy of applying a method with linear fundamentals to nonlinear problems was examined. It is observed that if the magnitude of nonlinearity is less than 1,000 times that of the nominal linear response, the error associated with applying successive linearization will result in 1σ errors in the response less than 10% compared to the full nonlinear error.

Nomenclature

$\boldsymbol{\beta}$	Deterministic input contribution in the fixed-point iteration equation, $\boldsymbol{\beta} \in \mathbb{R}^{m\times d}$
$\boldsymbol{\delta}$	Bias in the fixed-point iteration equation, $\boldsymbol{\delta} \in \mathbb{R}^{m}$
$\boldsymbol{\gamma}$	Probabilistic input contribution in the fixed-point iteration equation, $\boldsymbol{\gamma} \in \mathbb{R}^{m\times p}$
$\boldsymbol{\Lambda}$	State contribution in the fixed-point iteration equation, $\boldsymbol{\Lambda} \in \mathbb{R}^{m\times m}$
$\boldsymbol{\lambda}$	Lagrange multiplier
$\boldsymbol{\Sigma}$	Covariance matrix
$\mathbf{A_j}$	Matrix describing the state contribution of the j^{th} contributing analysis, $\mathbf{A_j} \in \mathbb{R}^{l_j\times m}$
$\mathbf{B_j}$	Matrix describing the deterministic input contribution of the j^{th} contributing analysis, $\mathbf{B_j} \in \mathbb{R}^{l_j\times d}$
$\mathbf{C_j}$	Matrix describing the probabilistic input contribution of the j^{th} contributing analysis, $\mathbf{C_j} \in \mathbb{R}^{l_j\times p}$
$\mathbf{d_j}$	Bias associated with the j^{th} contributing analysis, $\mathbf{d_j} \in \mathbb{R}^{l_j}$
$\mathbf{I_{n\times n}}$	The $n \times n$ identity matrix
$\mathbf{u_d}$	Deterministic system-level inputs into the design, $\mathbf{u_d} \in \mathbb{R}^{d}$
$\mathbf{u_p}$	Probabilistic system-level inputs into the design, $\mathbf{u_p} \in \mathbb{R}^{p}$
$\mathbf{y_j}$	Contributing analysis output, $\mathbf{y_j} \in \mathbb{R}^{l_j}$
$\mathcal{N}(\boldsymbol{\mu}, \boldsymbol{\Sigma})$	Normal random variable with mean $\boldsymbol{\mu}$ and covariance $\boldsymbol{\Sigma}$
$\mathcal{N}(\mu, \sigma^2)$	Normal random variable with mean μ and variance σ^2
$\mathcal{O}$	Big-O complexity
$\mathcal{U}(x_{\min}, x_{\max})$	Uniform random variable which varies between $x_{\min}$ and $x_{\max}$
$\Re(\cdot)$	Real part of $(\cdot)$
$\tilde{(\cdot)}$	Nominal value of $(\cdot)$
d	Dimensionality of the deterministic inputs, *i.e.*, $d = \dim(\mathbf{u_d})$
$L(\cdot)$	Lagrangian
n	Number of contributing analyses

*Graduate Research Assistant, Guggenheim School of Aerospace Engineering, AIAA Student Member
†David and Andrew Lewis Professor of Space Technology, Guggenheim School of Aerospace Engineering, AIAA Fellow

p	Dimensionality of the probabilistic inputs, *i.e.*, $d = \dim(\mathbf{u_p})$
q	Order of the contributing analyses
r	Order of the response

I. Introduction

References 1–4 offer a new perspective on multidisciplinary design optimization (MDO), one that views the problem as a dynamical system. Viewing the MDO problem as a dynamical system is tractable as the problem can be thought of as a multidimensional root-finding problem. In turn, the iteration scheme has been shown to meet the requirements of a dynamical system. Viewing the MDO problem as a dynamical system enables a rapid robust design methodology as described and applied in Refs. 1 and4. The linearity assumption is necessary in order to apply a Kalman filter in a method analogous to that in linear covariance analysis to obtain robustness characteristics.[5–7] Since the Kalman filter has linear roots, successive linearization is required to apply it to nonlinear problems. While it has been demonstrated that 1σ errors resulting from this approximation are less than 10% when applied to practical problems, the full extensibility of this linear methodology has not been explored.[1,4] This study investigates the extensibility of the rapid robust design methodology from both a computational and accuracy perspective and compares it to other traditional techniques.

II. Multidisciplinary Design as a Dynamical System

II.A. Identification of Feasible Designs

Identifying feasible designs in multidisciplinary systems can be thought of as the process of finding the root of a function. Consider a multidisciplinary problem where the analysis variables are described by a multivariable function $\mathbf{f}(\mathbf{u},\mathbf{p})$ where $\mathbf{u}$ are the design variables and $\mathbf{p}$ are the parameters of the problem. Assume that the requirements of the design are given by only equality constraints that are a function of the performance of the system. The performance of the design is described by a multi-variable mapping $\mathbf{g}(\mathbf{f}(\mathbf{u},\mathbf{p}))$ and the requirements are given by $\mathbf{z}$. In order to meet the requirements it is necessary to adjust the design variables $\mathbf{u}$ so that

$$\mathbf{z} = \mathbf{g}(\mathbf{f}(\mathbf{u},\mathbf{p})) \tag{1}$$

The solution $\mathbf{u}^*$ of Eq. (1) is the root of the system. Since identifying feasible designs within the multidisciplinary design problem requires finding the value of $\mathbf{u}$ that satisfies Eq. (1), this process can be thought of as a root-finding problem when an iterative solution method is chosen.

Many numerical methods for finding the root of a function, $\mathbf{g}(\mathbf{u})$, are dynamical systems since they rely on iterative schemes to identify the root.[8] For instance, the bisection method, secant method, function iteration method, and Newton's method are all iterative techniques that satisfy the requirements of a dynamical system.

II.B. Design Optimization

In order for a converged design to be an optimum with respect to some objective function, its performance needs to be evaluated with respect to other potential designs. The general optimization problem is formulated as

$$\left.\begin{array}{lll} \textbf{Minimize}: & \mathcal{J}(\mathbf{u},\mathbf{p}) & \\ \textbf{Subject to}: & \mathbf{g}_i(\mathbf{u},\mathbf{p}) \leq \mathbf{0}, & i = 1,\ldots,n_g \\ & \mathbf{h}_j(\mathbf{u},\mathbf{p}) = \mathbf{0}, & j = 1,\ldots,n_h \\ \textbf{By varying}: & \mathbf{u} & \end{array}\right\} \tag{2}$$

which requires a stationary point of the Lagrangian given as

$$L(\mathbf{u},\mathbf{p},\boldsymbol{\lambda}) = \mathcal{J}(\mathbf{u},\mathbf{p}) + \sum_{i=1}^{n_g} \lambda_i \mathbf{g}_i(\mathbf{u},\mathbf{p}) + \sum_{j=1}^{n_h} \lambda_{n_g+j} \mathbf{h}_j(\mathbf{u},\mathbf{p}) \tag{3}$$

to be found. The stationary point of the Lagrangian (Eq. (3)) is the value of $\mathbf{u}$ such that $\nabla_{\mathbf{u}} L(\mathbf{u},\mathbf{p},\boldsymbol{\lambda}) = \mathbf{0}$.

II.C. Identifying an Optimal Multidisciplinary Design

Multidisciplinary design optimization can be broken down into two steps: (1) identifying feasible designs and (2) identifying the optimal design from the set of feasible candidates. As discussed, both of these steps are root-finding problems. With the choice of an appropriate iterative numerical root-finding scheme, each of these individual steps can be posed as dynamical systems. When combined together, a nested root-finding problem results.

III. A Rapid Robust Multidisciplinary Design Methodology

A methodology that rapidly obtains the mean and a bound on the variance of a multidisciplinary design was developed in Ref.1. This new methodology treats the multidisciplinary design problem as a dynamical system. Viewing the multidisciplinary design problem as a dynamical system enables stability, control, and estimation techniques from dynamical system theory to be applied in order to rapidly obtain a robust optimal design.[1]

III.A. Procedure

Ref. 1 provides a rigorous description and derivation of the steps of the rapid robust design methodology which are summarized below.

1. **Decompose the design**: A general multidisciplinary design can be decomposed into multiple contributing analyses (CAs). Each of these CAs represents an analysis that contributes to the entire design. In the theoretical development underlying Ref. 1, it is assumed that each of the CAs are linear and algebraic, where the output of each of the CAs is of the form

$$\mathbf{y_j} = \mathbf{A_j y} + \mathbf{B_j u_d} + \mathbf{C_j u_p} + \mathbf{d_j} \tag{4}$$

   where $\mathbf{y}$ is the concatenated output from all of the CAs, $\mathbf{u_d}$ are the deterministic system-level inputs into the design, $\mathbf{u_p}$ are the probabilistic system-level inputs into the design, and $\mathbf{d_j}$ is the bias associated with the model.

   For general designs where the CAs may not be linear, the required functional form can be achieved through linearization where $\mathbf{A_j} = \left.\frac{\partial \mathbf{g}}{\partial \mathbf{y}}\right|_{\tilde{\mathbf{y}}}$, $\mathbf{B_j} = \left.\frac{\partial \mathbf{g}}{\partial \mathbf{u_d}}\right|_{\tilde{\mathbf{u}}_\mathbf{d}}$, $\mathbf{C_j} = \left.\frac{\partial \mathbf{g}}{\partial \mathbf{u_p}}\right|_{\tilde{\mathbf{u}}_\mathbf{p}}$, and $\mathbf{d_j} = -\left(\mathbf{A_j}\tilde{\mathbf{y}} + \mathbf{B_j}\tilde{\mathbf{u}}_\mathbf{d} + \mathbf{C_j}\tilde{\mathbf{u}}_\mathbf{p}\right)$ when the input-output relationship for the CA is given by $\mathbf{y_j} = \mathbf{g}\left(\mathbf{y}, \mathbf{u_d}, \mathbf{u_p}\right)$ and $\tilde{(\cdot)}$ is the value of $(\cdot)$ about which the function is linearized. During the iteration, $\tilde{(\cdot)}$ is the value of $(\cdot)$ from the prior iteration.

2. **Identify the random variables in the design and their distributions**: To propagate the uncertainties associated with the parameters of the design through the design to estimate the robustness, the probabilistic variables must be identified. The random variables associated with the uncertainty within the design are handled in two different ways depending on where the random variable is functionally located. If the uncertainities are associated with the parameters of the design they are propagated through the covariance estimation of the Kalman filter. On the other hand, if the uncertainties are associated with the CAs, they are propagated through the bias term of the filter equations.

3. **Form the iterative equations**: In order to implement this methodology, a causal, discrete dynamical system must be formed. Assuming fixed-point iteration is used to converge the design, the dynamical system is given by

$$\mathbf{y}_k = \mathbf{\Lambda y}_{k-1} + \boldsymbol{\beta}\mathbf{u_d} + \boldsymbol{\gamma}\mathbf{u_p} + \boldsymbol{\delta} \tag{5}$$

   where $\mathbf{\Lambda} = \left(\mathbf{A_1}^T \ \cdots \ \mathbf{A_n}^T\right)^T$, $\boldsymbol{\beta} = \left(\mathbf{B_1}^T \ \cdots \ \mathbf{B_n}^T\right)^T$, $\boldsymbol{\gamma} = \left(\mathbf{C_1}^T \ \cdots \ \mathbf{C_n}^T\right)^T$, and $\boldsymbol{\delta} = \left(\mathbf{d_1}^T \ \cdots \ \mathbf{d_n}^T\right)^T$.

4. **Ensure a solution exists**: Since the iterative system defined by Eq. (5) is a discrete, linear, dynamical system, the existence of a solution to the multidisciplinary design problem is given solely by the stability

of the system. When successive linearization is required to make a nonlinear system fit the form required in Eq. (5), Lyapunov techniques can be employed. Methods to identify the convergence characteristics for both classes of designs are described in Ref. 2.

5. **Estimate the mean output and the covariance of the design**: The mean output of the multidisciplinary system and the associated covariance matrix are found by propagating the Kalman filter equations until convergence. In order to accomplish this, the iterative system formed in Eq. (5) needs to be transformed to the form needed by the Kalman filter by making the following substitutions

$$\mathbf{F}_{k-1} = \mathbf{\Lambda}, \quad \forall k \in \{1, 2, ...\} \tag{6}$$

$$\mathbf{B}_{k-1} = \begin{pmatrix} \boldsymbol{\beta} & \boldsymbol{\gamma} & \mathbf{I_{m\times m}} \end{pmatrix}, \quad \forall k \in \{1, 2, ...\} \tag{7}$$

$$\mathbf{u}_{k-1} = \begin{pmatrix} \mathbf{u_d}^T & \mathbf{u_p}^T & \boldsymbol{\delta}^T \end{pmatrix}^T, \quad \forall k \in \{1, 2, ...\} \tag{8}$$

The iterates are then found by by propagating the filter equations until the design convergence criterion is met.

6. **Identify the mean and variance bound of the objective function**: The mean and variance of the design objective (*e.g.*, the 1σ accuracy or 1σ range) are found from the last iterate of the Kalman filter propagation. Where the mean value is taken directly from the filter value and a bound on the variance is found by applying the matrix 2-norm to the covariance matrix.

7. **Optimize for uncertainty and ensure constraints are met**: An optimal control problem can be setup where it is desired to find control, $\mathbf{u}$, that minimizes a weighted function of the mean and variance of the response. A solution to this optimal control problem is described in Ref. 3.

IV. A Linear, Two Contributing Analysis Design

The accuracy and computational speed of the rapid robust design methodology are first demonstrated by using the coupled, linear two CA system is shown in Fig. 1. For this analysis, assume that there are two

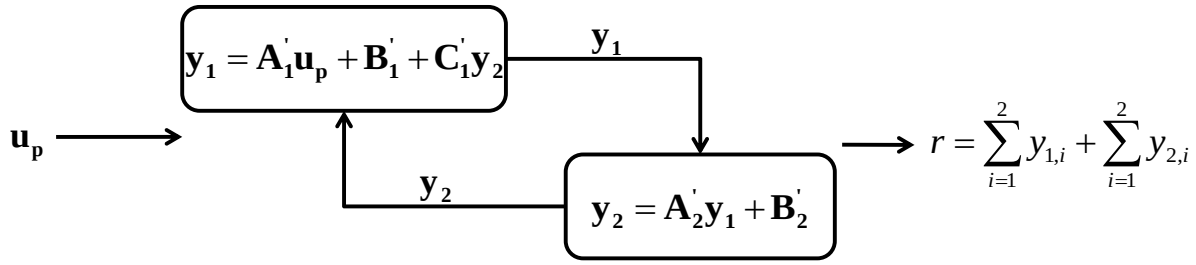

Figure 1. Two-contributing analysis multidisciplinary design.

components to the probabilistic parameter vector and the two output vectors, that is $\mathbf{u_p} \in \mathbb{R}^2$, $\mathbf{y_1} \in \mathbb{R}^2$, and $\mathbf{y_2} \in \mathbb{R}^2$, which, in turn, implies $\mathbf{A_1'} \in \mathbb{R}^{2\times 2}$, $\mathbf{B_1'} \in \mathbb{R}^2$, $\mathbf{C_1'} \in \mathbb{R}^{2\times 2}$, $\mathbf{A_2'} \in \mathbb{R}^{2\times 2}$, and $\mathbf{B_2'} \in \mathbb{R}^2$. Also, let the distribution of the probabilistic parameter input be given by a multivariate normal, $\mathbf{u_p} \sim \mathcal{N}(\boldsymbol{\mu}_{\mathbf{u_p}}, \boldsymbol{\Sigma}_{\mathbf{u_p}})$.

The effectiveness of the rapid robustness assessment methodology (*i.e.*, Steps 1 - 5 of the rapid robust design methodology described) will be demonstrated by letting the mean of the probabilistic input, $\boldsymbol{\mu}_{\mathbf{u_p}}$, and the components of the covariance matrix $\sigma_{y_1}^2$, $\sigma_{y_2}^2$, and $\rho_{y_1 y_2}$ vary between given ranges. The maximum error between the response obtained from the robustness assessment methodology and an analytical propagation is then reported for a multitude of points within the design space.

IV.A. Analytical Solution

As this is a multidisciplinary analysis consisting of two linear CAs, there is a single simultaneous solution for $\mathbf{y_1}$ and $\mathbf{y_2}$ which is found to be

$$\left.\begin{array}{rcl} \mathbf{y_1} &=& \left(\mathbf{I_{2\times 2}} - \mathbf{C_1'A_2'}\right)^{-1}\left(\mathbf{A_1'u_p} + \mathbf{B_1'} + \mathbf{C_1'B_2'}\right) \\ \mathbf{y_2} &=& \mathbf{A_2'}\left(\mathbf{I_{2\times 2}} - \mathbf{C_1'A_2'}\right)^{-1}\left(\mathbf{A_1'u_p} + \mathbf{B_1'} + \mathbf{C_1'B_2'}\right) + \mathbf{B_2'} \end{array}\right\}$$

which implies that whenever $\mathbf{I_{2\times 2}} - \mathbf{C_1'A_2'}$ is non-singular, a unique solution exists for $\mathbf{y_1}$ and $\mathbf{y_2}$. Since the only uncertainty in this analysis is given by the probabilistic input vector, $\mathbf{u_p}$, which is defined as a multivariate normal, the distribution of the output for each CA can be found exactly. These are given by

$$\left.\begin{array}{rcl} \mathbf{y_1} &\sim& \mathcal{N}\left(\boldsymbol{\mu}_{\mathbf{y_1}}, \boldsymbol{\Sigma}_{\mathbf{y_1}}\right) \\ \mathbf{y_2} &\sim& \mathcal{N}\left(\boldsymbol{\mu}_{\mathbf{y_2}}, \boldsymbol{\Sigma}_{\mathbf{y_2}}\right) \end{array}\right\}$$

where

$$\begin{array}{rcl} \boldsymbol{\mu}_{\mathbf{y_1}} &=& \left(\mathbf{I_{2\times 2}} - \mathbf{C_1'A_2'}\right)^{-1}\mathbf{A_1'}\boldsymbol{\mu}_{\mathbf{u_p}} + \left(\mathbf{I_{2\times 2}} - \mathbf{C_1'A_2'}\right)^{-1}\left(\mathbf{B_1'} + \mathbf{C_1'B_2'}\right) \\ \boldsymbol{\Sigma}_{\mathbf{y_1}} &=& \left(\mathbf{I_{2\times 2}} - \mathbf{C_1'A_2'}\right)^{-1}\mathbf{A_1'}\boldsymbol{\Sigma}_{\mathbf{u_p}}\mathbf{A_1'}^{T}\left(\mathbf{I_{2\times 2}} - \mathbf{C_1'A_2'}\right)^{-T} \end{array}$$

and

$$\begin{array}{rcl} \boldsymbol{\mu}_{\mathbf{y_2}} &=& \mathbf{A_2'}\left(\mathbf{I_{2\times 2}} - \mathbf{C_1'A_2'}\right)^{-1}\mathbf{A_1'}\boldsymbol{\mu}_{\mathbf{u_p}} + \mathbf{A_2'}\left(\mathbf{I_{2\times 2}} - \mathbf{C_1'A_2'}\right)^{-1}\left(\mathbf{B_1'} + \mathbf{C_1'B_2'}\right) + \mathbf{B_2'} \\ \boldsymbol{\Sigma}_{\mathbf{y_2}} &=& \mathbf{A_2'}\left(\mathbf{I_{2\times 2}} - \mathbf{C_1'A_2'}\right)^{-1}\mathbf{A_1'}\boldsymbol{\Sigma}_{\mathbf{u_p}}\mathbf{A_1'}^{T}\left(\mathbf{I_{2\times 2}} - \mathbf{C_1'A_2'}\right)^{-T}\mathbf{A_2'}^{T} \end{array}$$

Since both of the output distributions from the CAs are also multivariate normal, the components of the response

$$r = \sum_{i=1}^{2} y_{1,i} + \sum_{i=1}^{2} y_{2,i}$$

can be found exactly by summing the components of mean components of $\boldsymbol{\mu}_{\mathbf{y_1}}$ and $\boldsymbol{\mu}_{\mathbf{y_2}}$ to find the mean of the response and adding the appropriate variances from the covariance matrices $\boldsymbol{\Sigma}_{\mathbf{y_1}}$ and $\boldsymbol{\Sigma}_{\mathbf{y_2}}$. That is

$$r \sim \mathcal{N}\left(\sum_{i=1}^{2}\boldsymbol{\mu}_{\mathbf{y_1},i} + \sum_{i=1}^{2}\boldsymbol{\mu}_{\mathbf{y_2},i}, \sum_{i=1}^{2}\lambda(\boldsymbol{\Sigma}_{\mathbf{y_1}})|_i + \sum_{i=1}^{2}\lambda(\boldsymbol{\Sigma}_{\mathbf{y_2}})|_i\right)$$

where $\boldsymbol{\mu}_{\mathbf{y_1},i}$ is the i^{th} component of $\mathbf{y_1}$, $\boldsymbol{\mu}_{\mathbf{y_2},i}$ is the i^{th} component of $\mathbf{y_2}$, and $\lambda(\cdot)|_i$ is the i^{th} eigenvalue of the matrix argument.

IV.B. Analysis Results

IV.B.1. Accuracy with Respect to Analytical Propagation

In order to assess a large variety of problems, a parametric sweep of the design variables was performed to identify the maximum errors in the design space. To perform this parameter sweep, the problem's parameters were varied independently as shown in Table 1 where the distribution of each variable was assumed to be uniform and a 100,000 case Monte Carlo analysis was conducted.

Table 1. Parameter ranges to assess the validity of the rapid robust design methodology.

Parameter	Distribution
σ_1^2	$\mathcal{U}(0,100)$
σ_2^2	$\mathcal{U}(0,100)$
$\rho_{y_1 y_2}$	$\mathcal{U}(-1,1)$
$\mathbf{A_1'}$	$\begin{pmatrix}\mathcal{U}(-1,1) & \mathcal{U}(-1,1)\\ \mathcal{U}(-1,1) & \mathcal{U}(-1,1)\end{pmatrix}$
$\mathbf{B_1'}$	$\begin{pmatrix}\mathcal{U}(-1,1)\\ \mathcal{U}(-1,1)\end{pmatrix}$
$\mathbf{C_1'}$	$\begin{pmatrix}\mathcal{U}(-1,1) & \mathcal{U}(-1,1)\\ \mathcal{U}(-1,1) & \mathcal{U}(-1,1)\end{pmatrix}$
$\mathbf{A_2'}$	$\begin{pmatrix}\mathcal{U}(-1,1) & \mathcal{U}(-1,1)\\ \mathcal{U}(-1,1) & \mathcal{U}(-1,1)\end{pmatrix}$
$\mathbf{B_2'}$	$\begin{pmatrix}\mathcal{U}(-1,1)\\ \mathcal{U}(-1,1)\end{pmatrix}$

In order to guarantee convergence of the design, constraints were imposed on the parameters to ensure that all of the eigenvalues of the matrix $\mathbf{\Lambda}$ had modulus less than unity. To ensure realizable covariance matrices, that is a matrix that is symmetric and positive definite, the components of the covariance (*e.g.*, variance and correlation coefficient) were determined independently and then combined to form the covariance matrix. The results of this propagation were then compared with results propagated analytically resulting in Figs. 2. It is observed from these results that the mean error is less than 0.08% for all of the cases examined. This is a result of the system being linear and the Kalman filter propagating results exactly for a linear system. Therefore the error in the mean is solely a result of the convergence criterion being utilized. For each case, there is seen to be a rise in the standard deviation error near the origin. This is because the nominal mean goes to zero causing a rise in the in the percent error near this point.

The rapid robustness assessment methodology is observed to provide a consistent conservative bound on the variance as all of the percent error values are positive. It is also interesting to note that the error in mean and standard deviation appears to be close to the same order of magnitude. Furthermore, it is observed that the maximum error approaches a limit of less than 40%. This limit is a function of the two-norm being used. In analyzing the data, the largest errors are caused for weakly coupled systems, that is systems where $\mathbf{C_1'}$ is small. This can be explained since $\mathbf{C_1'}$ being small leads to a larger domain of values that lead to a converged design. Additionally, since the interplay between $\mathbf{y_1}$ and $\mathbf{y_2}$ is reduced, the iterations to achieve convergence is reduced in these cases.

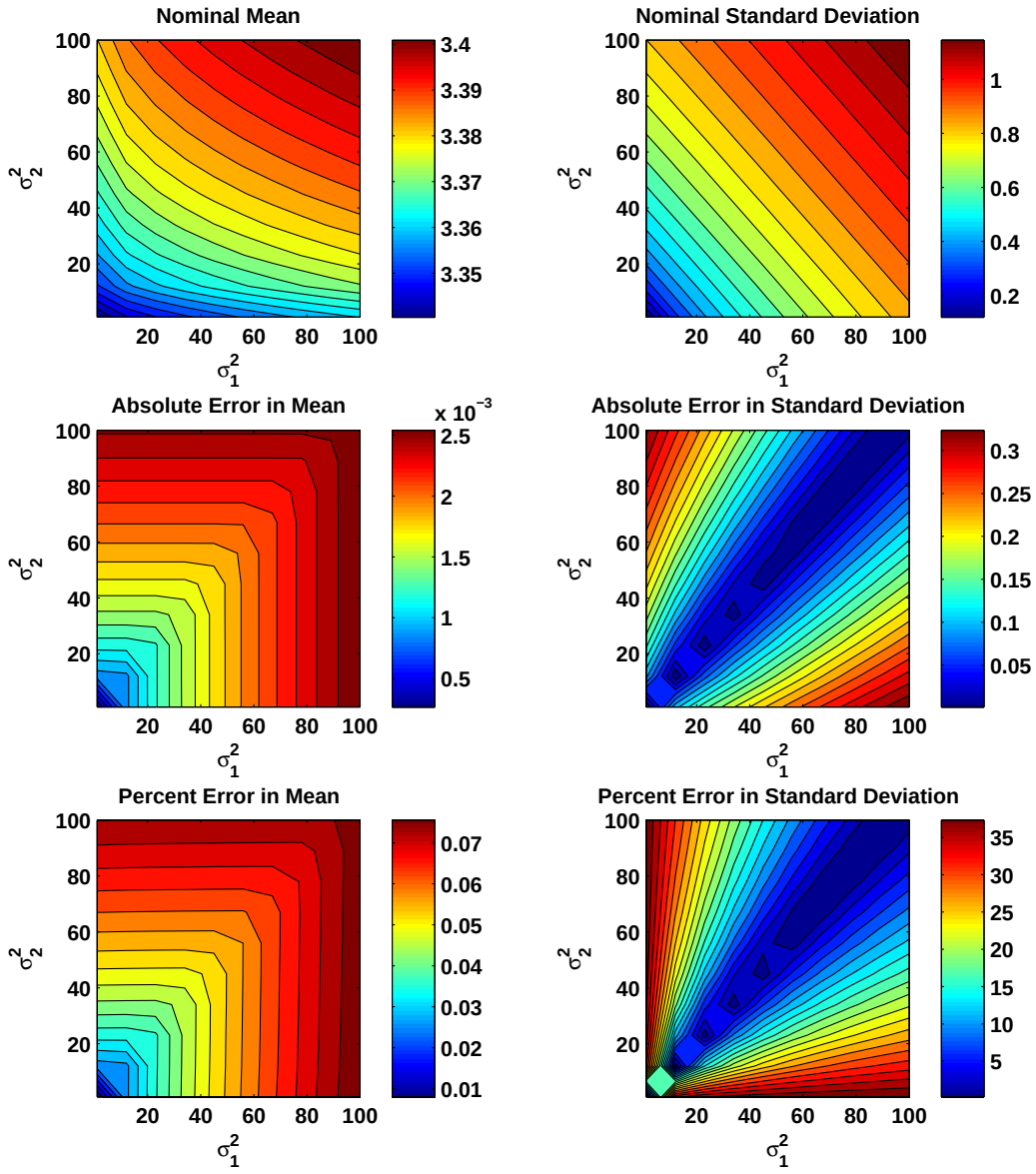

Figure 2. Maximum error for a two contributing analysis multidisciplinary design with $\mu_{\mathbf{u_p}} = (0\ 0)^T$.

IV.B.2. Computational Comparison with Traditional Techniques

The errors associated with the rapid linear robustness technique are compared to more commonly used methods to propagate uncertainty, namely a 10,000 case Monte Carlo analysis, the unscented transform, and fast probability integration. For the data presented, specific numerical values were utilized for the various problem matrices and vectors. These are given by

$$\mathbf{A'_1} = \begin{pmatrix} 0.25 & 0 \\ 0 & 0.5 \end{pmatrix} \quad \mathbf{B'_1} = \begin{pmatrix} 1 \\ 1 \end{pmatrix} \quad \mathbf{C'_1} = \begin{pmatrix} 1 & 0 \\ 0 & 1 \end{pmatrix}$$

$$\mathbf{A_2'} = \begin{pmatrix} 0.25 & 0 \\ 0 & 0.25 \end{pmatrix} \quad \mathbf{B_2'} = \begin{pmatrix} 1 \\ 1 \end{pmatrix}$$

The advantages of the rapid robust analysis technique are elucidated in the Table 2 where the four techniques are compared to analytic propagation of the uncertainty. This table reports the maximum error from a parameter sweep of $\sigma^2_{u_{p,1}}$, $\sigma^2_{u_{p,2}}$, and $\rho_{u_{p,1}u_{p,2}}$ across the range of values in Table 1 with $\boldsymbol{\mu}_{\mathbf{u_p}} = (0\ 0)^T$. It can be seen that the rapid robust analysis technique provides a slightly improved level of accuracy relative to the other contemporary methods in estimating the mean. The error in standard deviation is larger than the other techniques (three times greater than the unscented transform); however, this error is less than 3% and is acceptable for conceptual design studies. These levels of accuracy are obtained for less than one-third the number of CA evaluations compared to the unscented transform and orders of magnitude fewer CA evaluations relative to Monte Carlo and fast probability integration. For problems in which the CA function evaluation time is large or the model for each CA needs to be built in real-time, this provides a large execution time benefit.

Table 2. Comparison of the performance of the rapid robustness assessment method with other multidisciplinary uncertainty assessment techniques.

	Rapid Robust Design Methodology	**Monte Carlo**	**Unscented Transform**	**Fast Probability Integration**
Maximum Percent Discrepancy in Mean Relative to Analytic Propagation, %	0.07843	0.10234	0.18458	0.10357
Maximum Percent Discrepancy in Standard Deviation Relative to Analytic Propagation, %	2.4583	0.02939	0.80879	0.14299
Number of CA Evaluations, -	140	109,954	435	2,349

V. Computational Effect of Increasing the Design Complexity on the Rapid Robust Design Methodology

In Refs. 1 and 4 the use of the rapid robust design methodology on several example applications ranging from analytical problems to a problem relevant to the EDL community was demonstrated. For these problems, the number of function evaluations were reduced by a factor that approached thirty relative to traditional Monte Carlo methods wrapped in an evolutionary optimizer. The following sections examine the effect of design complexity on the number of function evaluations required to obtain a solution. Quantitatively defining the complexity of the design is a matter of debate amongst experts.[9–12] In this investigation *design complexity* is defined as the relative difficulty in obtaining an optimal design.

In this sense, design complexity is used in the structural sense.[11] In terms of the MDO problem, structural design complexity is comprised of components such as the number of design variables, the number of CAs, the nonlinearity of the CAs, and the nonlinearity of the response function. For the rapid robust design methodology developed in this work, the effect of each of these components are first examined individually, then several overall evaluation criterion are applied. Some of these overall evaluation criterion also evaluate the strength of coupling between the CAs.

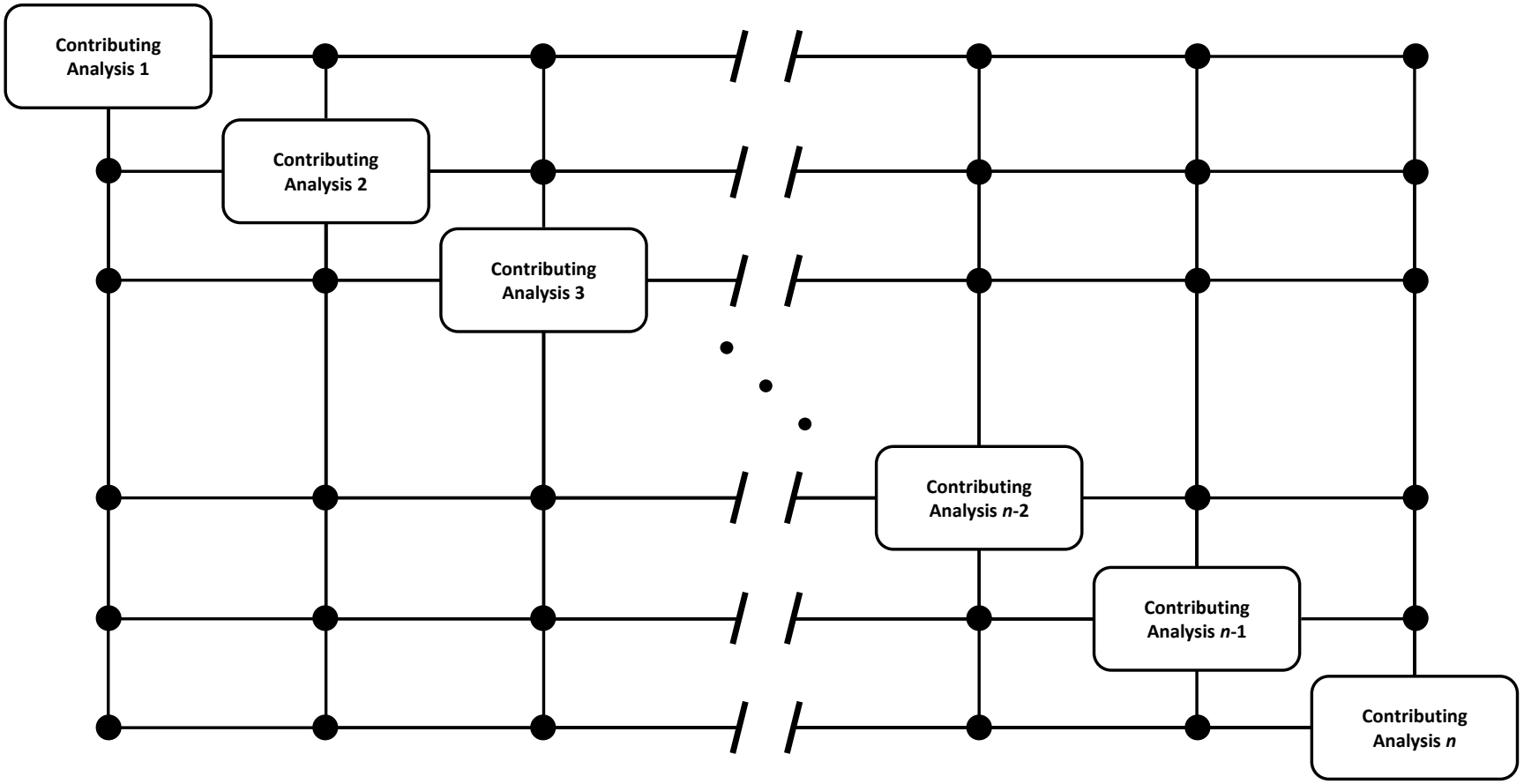

Figure 3. General design structure matrix for analyzing the effect of design complexity.

V.A. Test Problem Definition

To assess the effect of increasing design complexity on the computational efficiency of the rapid robust design methodology, a generalized test problem was formulated. This test problem is shown in Fig. 3. The DSM in Fig. 3 is fully coupled and can be functionally represented as

$$\mathbf{y}_i = \mathbf{f}(\mathbf{y}_1, \mathbf{y}_2, \cdots, \mathbf{y}_{i-1}, \mathbf{y}_{i+1}, \cdots, \mathbf{y}_{n-1}, \mathbf{y}_n, , \mathbf{u}) \tag{9}$$

where in this case $\mathbf{f}(\cdot)$ and each CA are scalar functions. The function in Eq. (9) is represented as an q^{th}-order polynomial

$$\begin{aligned}\mathbf{f}(\mathbf{y}_1,&\mathbf{y}_2, \cdots, \mathbf{y}_{i-1}, \mathbf{y}_{i+1}, \cdots, \mathbf{y}_{n-1}, \mathbf{y}_n, \mathbf{u}) = \\ &\sum_{j_1=1}^{q}\sum_{j_2=1}^{q}\cdots\sum_{j_{n-1}=1}^{q}\sum_{j_n=1}^{q}\left[a(j_1, j_2, \cdots j_{n-1}, j_n) y_1^{j_1} y_2^{j_2} \cdots y_{n-1}^{j_{n-1}} y_n^{j_n} + \sum_{i=1}^{d+p} u_i\right]\end{aligned} \tag{10}$$

Similarly, the response function is a r^{th}-order polynomial consisting of the outputs for each of the contributing analysis

$$r = \sum_{j_1=1}^{r}\sum_{j_2=1}^{r}\cdots\sum_{j_{n-1}=1}^{r}\sum_{j_n=1}^{r} b(j_1, j_2, \cdots j_{n-1}, j_n) y_1^{j_1} y_2^{j_2} \cdots y_{n-1}^{j_{n-1}} y_n^{j_n} \tag{11}$$

In each case the coefficients, are given by

$$a(j_1, j_2, \cdots j_{n-1}, j_n) = \begin{cases} \mathcal{U}(-1, 1), & j_i \neq i \\ 0, & j_i = i \end{cases} \tag{12}$$

and

$$b(j_1, j_2, \cdots j_{n-1}, j_n) \sim \mathcal{U}(-1, 1) \tag{13}$$

which are sampled before evaluating for each design. The inputs, $\mathbf{u} \in \mathbb{R}^{d+p}$, are prescribed by

$$u_i = \begin{cases} u_{d_i}, & i \leq d \\ \mathcal{N}(0, 100), & d < i \leq d + p \end{cases} \tag{14}$$

where u_{d_i} are assumed to be design variables, $d \geq 1$, and $p \geq 1$.

The unconstrained robust design problem is given by

$$\left.\begin{array}{ll} \textbf{Minimize}: & \mathcal{J} = \bar{r} + \sigma_r \\ \textbf{By varying}: & \mathbf{u_d} \end{array}\right\}$$

where $\bar{r}$ is the sample mean of r and σ_r is the sample standard deviation (or its estimate, $\sqrt{\| \mathbf{\Sigma_y} \|_2}$, in the case of the rapid robust design methodology).

V.B. Individual Sensitivities

The individual effect of the number of design variables, number of CAs, nonlinearity of the CAs, and nonlinearity of the response are discussed below. In each case the number of function evaluations is compared to a Newton-based solution where the uncertainties are provided by a Monte Carlo simulation, FPI, or unscented transform. In the case of the Monte Carlo, the number of samples was continually increased until the change in the variance estimate was less than 1%.

Table 3 shows the parameters used to analyze each scenario used when examining the individual effects of the increase in complexity while Fig. 4 shows the computational cost as each of these parameters are varied. For each sensitivity analysis, the number of probabilistic parameters, p, was fixed at 10.

Table 3. Parameters used to examine the individual effect of complexity parameters on the design.

Parameter	Description	Number of Design Variables	Number of CAs	CA Non-linearity	Response Nonlinearity
d	Number of design variables	Variable	1	1	1
n	Number of CAs	10	Variable	10	10
q	Order of the CAs	1	1	Variable	1
r	Order of the response	1	1	1	Variable

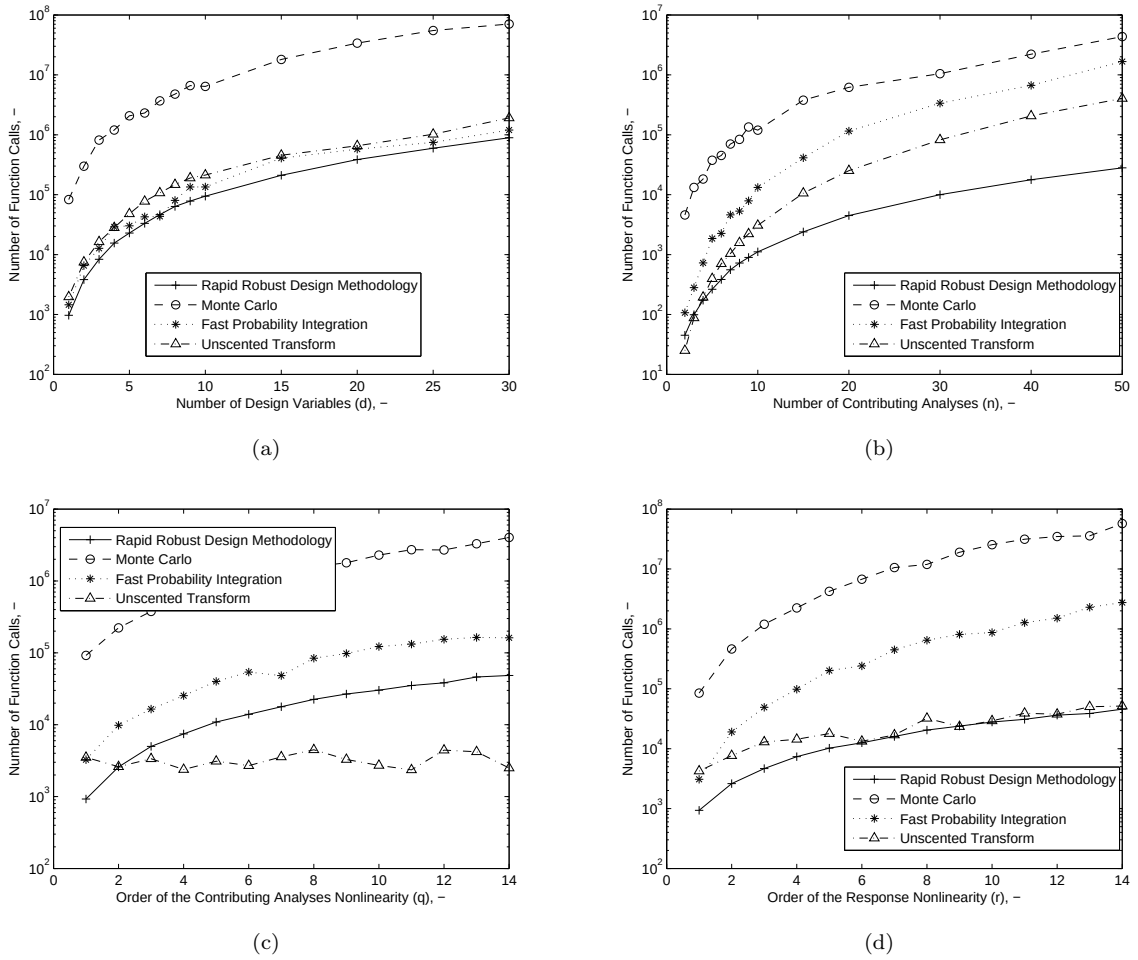

Figure 4. Increase in computational cost with (a) number of design variables, (b) number of contributing analyses, (c) nonlinearity of the CAs, and (d) nonlinearity of the response.

V.B.1. Effect of Number of Design Variables

In this case, the number of design variables, d, is varied while the other parameters were held constant as shown in Table 3. Figure 4(a) shows that each of the methods exhibit algebraic growth with number of

design variables (*i.e.*, the number of function calls goes as $\mathcal{O}(n^c)$ for some c). As a Newton optimization algorithm is being utilized, this is expected. It is also observed that the Monte Carlo solutions have an order of magnitude more function evaluations compared to the other techniques considered. This is expected since the rapid robust design methodology, FPI, and unscented transform require a fixed number of function evaluations to obtain the mean and the variance.

V.B.2. Effect of Number of Contributing Analyses

The number of CAs is representative of the complexity of the problem domain. To analyze this effect on the number of function calls, the number of CAs, n, is varied while the other parameters were held constant as shown in Table 3. As seen in Fig. 4(b), each of the methods exhibit approximately algebraic growth with the number of CAs. The increase in the number of function calls is a result of the fixed-point iteration requiring an increasing number of iterations in order to reach the convergence tolerance. For larger designs (greater than 20 CAs), the rate of function call growth with number of CAs is similar between each of the methods. However, for small designs (less than 20 CAs) the rapid robust design methodology is observed to have the slowest rate of growth.

V.B.3. Effect of Contributing Analysis Nonlinearity

The effect of CA nonlinearity was assessed by varying the maximum degree of the polynomial defined in Eq. (10), q. Each of the ten CAs' order is varied simultaneously so that each polynomial has the same number of terms. The other parameters used in this analysis are shown in Table 3. Figure 4(c) shows that the rapid robust design methodology and FPI again exhibit algebraic growth with the number of CAs due to the fact that they rely on successive linearization to approximate the system. Since the unscented transform does not depend on the linearity of the CAs and propagates the same number of samples based on the dimensionality of the problem $(n + d + p)$, it has no sensitivity to the nonlinearity of the CAs. The Monte Carlo exhibits algebraic growth initially, with exponential growth (*i.e.*, number of functions calls $\sim \mathcal{O}(c^q)$) for highly nonlinear systems. This can be attributed to the fact that the Monte Carlo simulation ensures that the change in the variance estimate is less than 1%, requiring additional sampling for more nonlinear designs.

V.B.4. Effect of Response Nonlinearity

The effect of response nonlinearity was assessed by varying the maximum degree of the polynomial defined in Eq. (11), r. The parameters used in this analysis are shown in Table 3 while the variation in the number of function calls required to obtain a robust design is shown in Fig. 4(d). The variation in the number of function calls required by the rapid robust design methodology and unscented transform as the response nonlinearity is increased is similar. Both of the techniques exhibit quasi-linear growth behavior for increasing nonlinearity, while the Monte Carlo and FPI exhibit an algebraic increase in the number of function calls.

V.C. Complexity Metrics

An overall complexity index could also be used to measure the performance of the rapid robust design methodology compared to traditional methods. Four different metrics are considered—an algebraic metric, a Jacobian metric, a force-based clustering metric, and an input-output graphical based metric. In addition providing information about the structure of the design problem, the Jacobian and the force based clustering metric also account for the functional relationship within the design. That is to say, in addition to topological considerations in the design, these metrics account for how strongly coupled the design is or what the mapping between the input and output looks like.

V.C.1. Algebraic Metric

The algebraic metric combines the four individual metrics discussed previously—the number of design variables, the number of CAs, the nonlinearity of the CAs, and the order of the response. The metric considered is defined as follows

$$\mathcal{C}_a = dr\left(\sum_{i=1}^{n} q_i\right) \tag{15}$$

where q_i is the order of the i^{th} CA. In this metric, the size and the order of the CAs are combined into a single value, the summation of the order of each CA; however, for a linear design, this reduces to the number of CAs.

V.C.2. Jacobian Metric

The Jacobian metric augments the algebraic metric with the addition of the order of the matrix of partial derivatives between the input and output of the design. Specifically, this metric is defined as

$$\mathcal{C}_J = \mathcal{C}_a \sum_{i=1}^{d} \mathcal{O}\left(\frac{\partial r}{\partial \mathbf{u_d}}\right)_i = dr\left(\sum_{i=1}^{n} q_i\right)\left(\sum_{i=1}^{d} \mathcal{O}\left(\frac{\partial r}{\partial \mathbf{u_d}}\right)_i\right) \tag{16}$$

The Jacobian captures the sensitivity of the output to perturbations in the input and is used in many optimization algorithms (*e.g.*, steepest-descent).

V.C.3. Force-Based Clustering Metric

Force-based clustering is a graphical method that can be used to reorder a design into a structured DSM and simultaneously provides information on the strength of the connection between CAs.[13] This method works by modeling the connections between CAs with an attractive force that clusters CAs with strong linkages, pulling CAs that use the same information together. Decomposing the problem in this way arranges the DSM in the "lowest energy" state, which can be used to measure the strength of the connections between the CAs. This complexity index augments the algebraic metric with the summation of these forces once the DSM is arranged in the minimal energy state.

$$\mathcal{C}_{fbc} = \mathcal{C}_a \mathcal{J}_{fbc} = dr \mathcal{J}_{fbc}\left(\sum_{i=1}^{n} q_i\right) \tag{17}$$

where $\mathcal{J}_{fbc}$ is the sum of the edges of the force-based clustering graph when decomposed.

V.C.4. Input-Output Graph Metric

The last metric considered is a graphical technique based on the topology of the design. In this method the net information flow through each CA is considered. That is the difference between the number of output variables to the number of used input variables is utilized,

$$\begin{aligned} \mathcal{C}_{io} &= \mathcal{C}_a \sum_{i=1}^{n} \left(\dim(\mathbf{y}_{i,\text{out}}) - \dim(\mathbf{y}_{i,\text{in}})\right) \\ &= dr\left(\sum_{i=1}^{n} q_i\right)\left(\sum_{i=1}^{n} \left(\dim(\mathbf{y}_{i,\text{out}}) - \dim(\mathbf{y}_{i,\text{in}})\right)\right) \end{aligned} \tag{18}$$

where $\mathbf{y}_{i,\text{out}}$ and $\mathbf{y}_{i,\text{in}}$ are the number of output variables and used input variables, respectively.

V.C.5. Correlation Between Cost and Complexity

The use of each of these techniques is demonstrated in Fig. 5 for nine representative designs. These designs varied from a linear, weakly coupled three CA system with a single input to a nonlinear design with 20 CAs, five design variables, and a highly nonlinear response. Each design case is shown in Table 4 where the number of probabilistic parameters, p, is assumed to be 5 for each case.

From Fig. 5, it is observed that the number of function calls generally increase for each metric. However, the number of function calls does not monotonically increase with the Jacobian augmented metric. Furthermore, as seen by the same complexity value resulting in multiple number of function calls, all metrics except force-based clustering provided multiple values for the number of function calls for low complexity designs. This makes the force-based clustering metric the most promising for evaluation of design complexity. However, this metric is also the most computationally intensive and requires the reorganization of the DSM. In cases where this is not tractable, the input-output metric is can be used as an alternative.

Table 4. Design cases used to evaluate the overall complexity metrics.

Parameter	Case 1	Case 2	Case 3	Case 4	Case 5	Case 6	Case 7	Case 8	Case 9
n	3	3	3	3	3	10	10	20	20
q	1	2	1	5	5	1	5	1	5
r	1	1	2	1	5	1	5	1	5
d	1	1	1	5	5	1	5	1	5

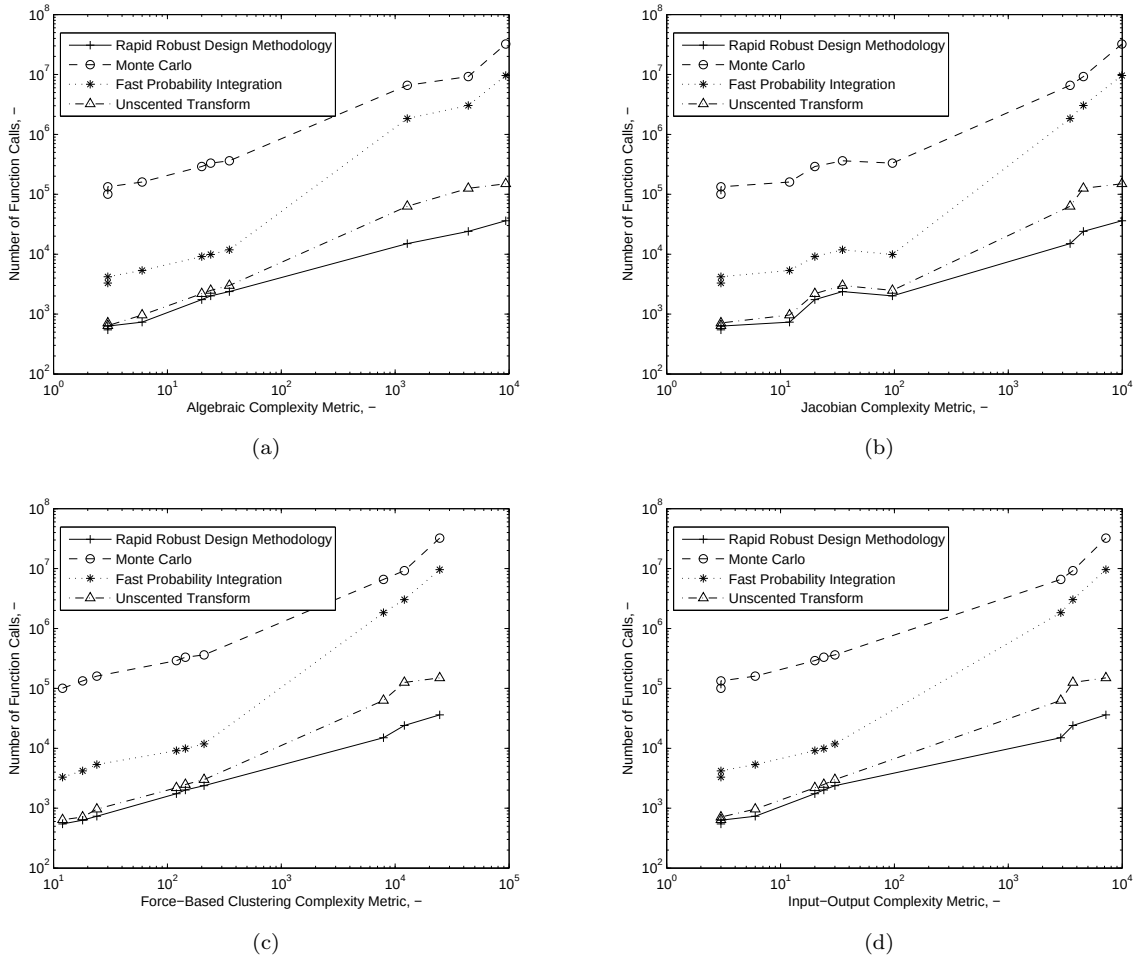

Figure 5. Increase in computational cost with complexities using the (a) algebraic complexity metric, (b) Jacobian complexity metric, (c) force-based clustering metric, and (d) input-output metric.

V.D. Computational Speed of the Rapid Robust Design Methodology

Figures 4 and 5 show favorable computational performance of the rapid robust design methodology compared to the more traditional design methodologies such as Monte Carlo simulation using a gradient-based optimization algorithm. The rapid robust design methodology scales favorably with the number of design variables and number of CAs, and its scaled performance was only met or exceeded by the unscented transform with respect to the nonlinearity of the CAs and response. Across the range of problems investigated, optimum designs were achieved using the rapid robust design methodology with fewer function calls than the traditional techniques evaluated with at least an order of magnitude less function evaluations compared to FPI and Monte Carlo methods). This implies that the rapid robust design methodology scales well with increasingly complex designs.

VI. The Accuracy of a Linear Technique

The rapid robust design methodology developed in this investigation is based on linear system theory. However, this methodology was extended to nonlinear problems through successive linearization as shown in Refs. 1, 4.

The extent of nonlinearity that the rapid robust design methodology can accommodate can be analyzed through a perturbation analysis. That is a nonlinearity is added to the converged linear system. This analysis is common in orbital mechanics and in control applications. For instance in orbital mechanics, this type of analysis is common when dealing with perturbations (*e.g.*, drag, gravity, etc.) in the Clohessy-Wilshire equations of relative motion.[14] For control applications, it is common to linearize around a trajectory and assess the effect of nonlinear perturbations to linear matrix propagation.[15]

For this analysis, two different designs were considered, one with three CAs and another with ten CAs. In each case the first $n-1$ CAs are scalar, linear, and fully coupled, while the last is assumed to be a scalar, linear function with a nonlinear perturbation term given by $g(\mathbf{y})$. This is shown in Figs. 6 and 7.

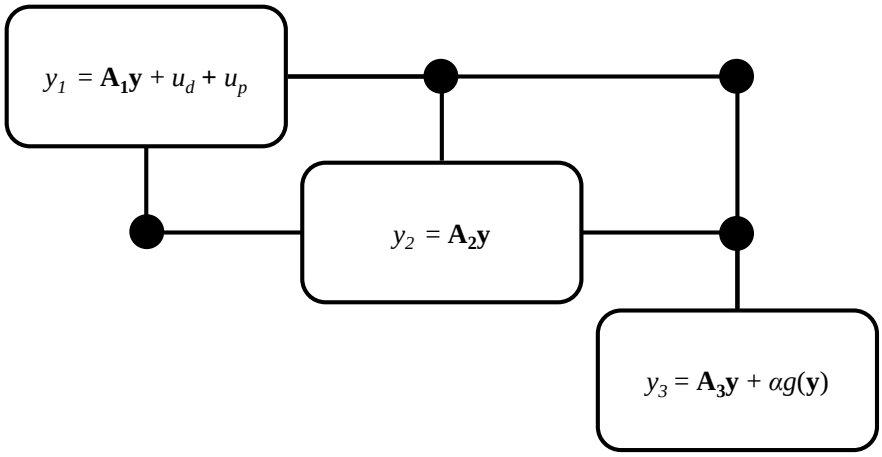

Figure 6. Three contributing analysis design structure matrix for nonlinearity analysis.

For these designs, the iteration equations (based on fixed-point iteration) is given by

$$\mathbf{y}_k = \mathbf{\Lambda y}_{k-1} + \boldsymbol{\beta}\mathbf{u_d} + \boldsymbol{\gamma}\mathbf{u_p} + \boldsymbol{\delta}_{k-1}$$

where

$$\mathbf{\Lambda} = \left(\mathbf{A_1}^T \ \cdots \mathbf{A_n}^T\right)^T$$

$$\boldsymbol{\beta} = \boldsymbol{\gamma} = \left(1\ 0\ \cdots\ 0\right)^T_{1\times n}$$

and

$$\boldsymbol{\delta} = \boldsymbol{\gamma} = \left(\alpha g(\mathbf{y}_{k-1})\ 0\ \cdots\ 0\right)^T_{n\times 1}$$

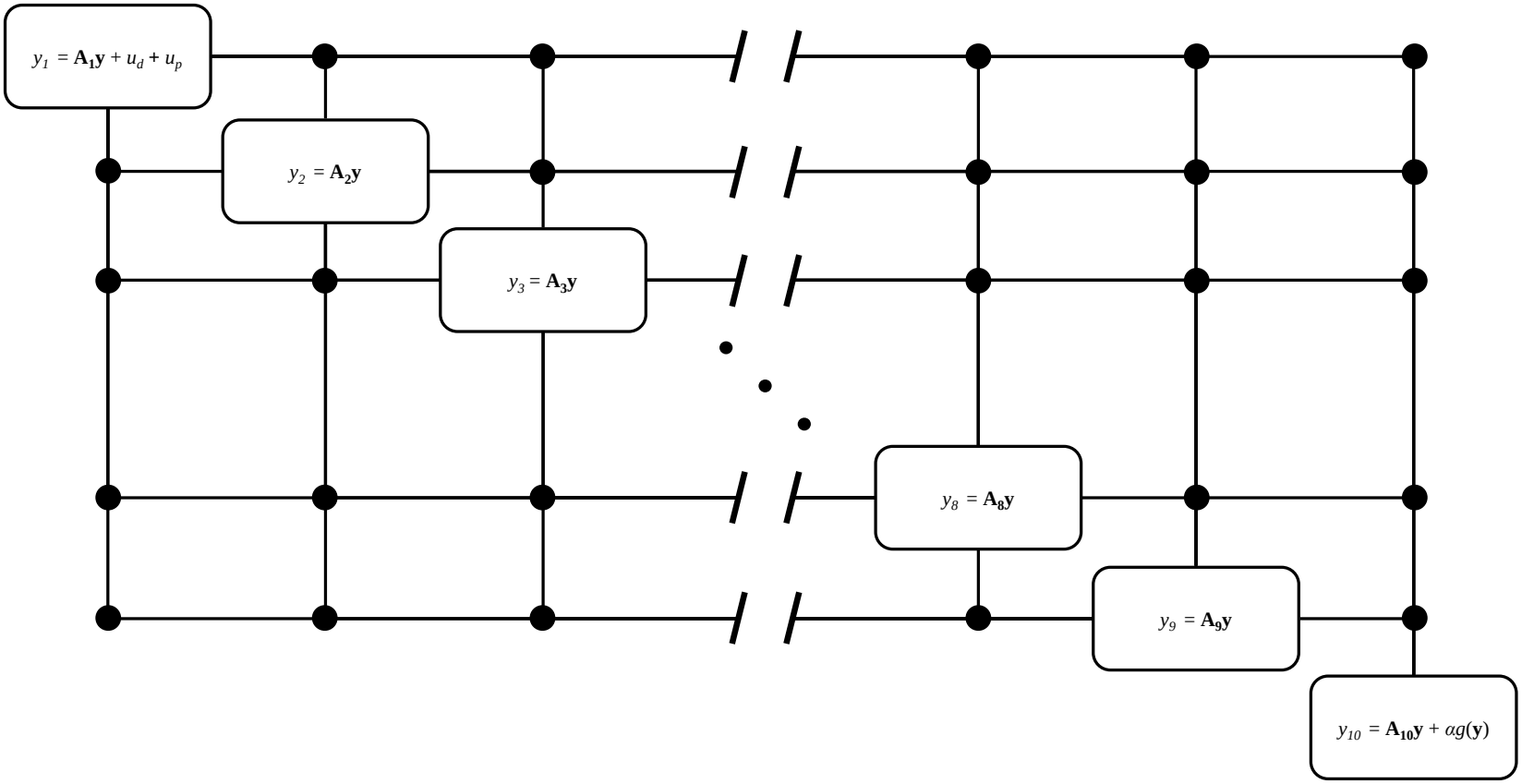

Figure 7. Ten contributing analysis design structure matrix for nonlinearity analysis

The values of $\mathbf{\Lambda}$ are given by

$$\mathbf{\Lambda}_{ij} = \begin{cases} 0, & i = j \text{ or } j = n \\ \frac{1}{2}, & \text{otherwise} \end{cases}$$

In addition, the inputs, $\mathbf{u} = (u_d \; u_p)^T \in \mathbb{R}^2$, are prescribed by

$$\begin{aligned} u_1 &= u_d \\ u_2 &\sim \mathcal{N}(0, 100) \end{aligned}$$

and the response is the value of the last CA,

$$r = y_n$$

Finally, the nonlinearity is prescribed by one of three different functions

$$g(\mathbf{y}) = \begin{cases} g_1(\mathbf{y}) = \sin\left(\sum_{i=1}^{n-1} y_i\right) \\ g_2(\mathbf{y}) = \ln\left(\sum_{i=1}^{n-1} y_i\right) \\ g_3(\mathbf{y}) = \Re(-1)^{\left(\sum_{i=1}^{n-1} y_i\right)} \end{cases}$$

Solutions to the robust optimization problem given by

$$\left.\begin{array}{ll} \textbf{Minimize}: & \mathcal{J} = \bar{y}_n + \sigma_{y_n} \\ \textbf{Subject to}: & y_i \geq 1 \quad \forall i \in \{1, \ldots, n\} \\ \textbf{By varying}: & u_d \end{array}\right\}$$

are found using a gradient based optimizer. In this problem, since there is only one probabilistic variable the two-norm provides directly the variance of the response used (*i.e.*, $\sigma_r = \sqrt{\| \mathbf{\Sigma} \|_2}$).

A solution is first found for a fully linear design (*i.e.*, $\alpha = 0$), y^*_{lin}. The weight on the nonlinearity is then varied to obtain the results seen in Fig. 8.

In Fig. 8, the error, defined as the percent difference in $\mathcal{J}$ between the Monte Carlo solution after the variance difference is less than 1% and the rapid robust design methodology, is plotted on a log-log plot as a function of ϵ

$$\epsilon = \frac{\alpha}{|y^*_{lin}|}$$

a normalized value of the perturbation. This normalized value of the perturbation can be thought of as an amplitude relative to nominal design response.

The analysis shows a consistent trend, once the amplitude of the nonlinearity is of the same order as the nominal response (*i.e.*, $\epsilon \sim 1$), the error increases significantly and once it is more than three orders of magnitude the error is greater than 10%. However, after this divergence point, the rate of growth of the error is similar to that prior to the divergence point. This result is independent of the size of the design and the perturbation function. Therefore, to keep the errors associated with the rapid robust design methodology consistent with that expected in the conceptual design phase (*i.e.*, $< 10\%$), one must keep the nonlinear part of the analysis to less than three orders of magnitude relative to the nominal linear response.

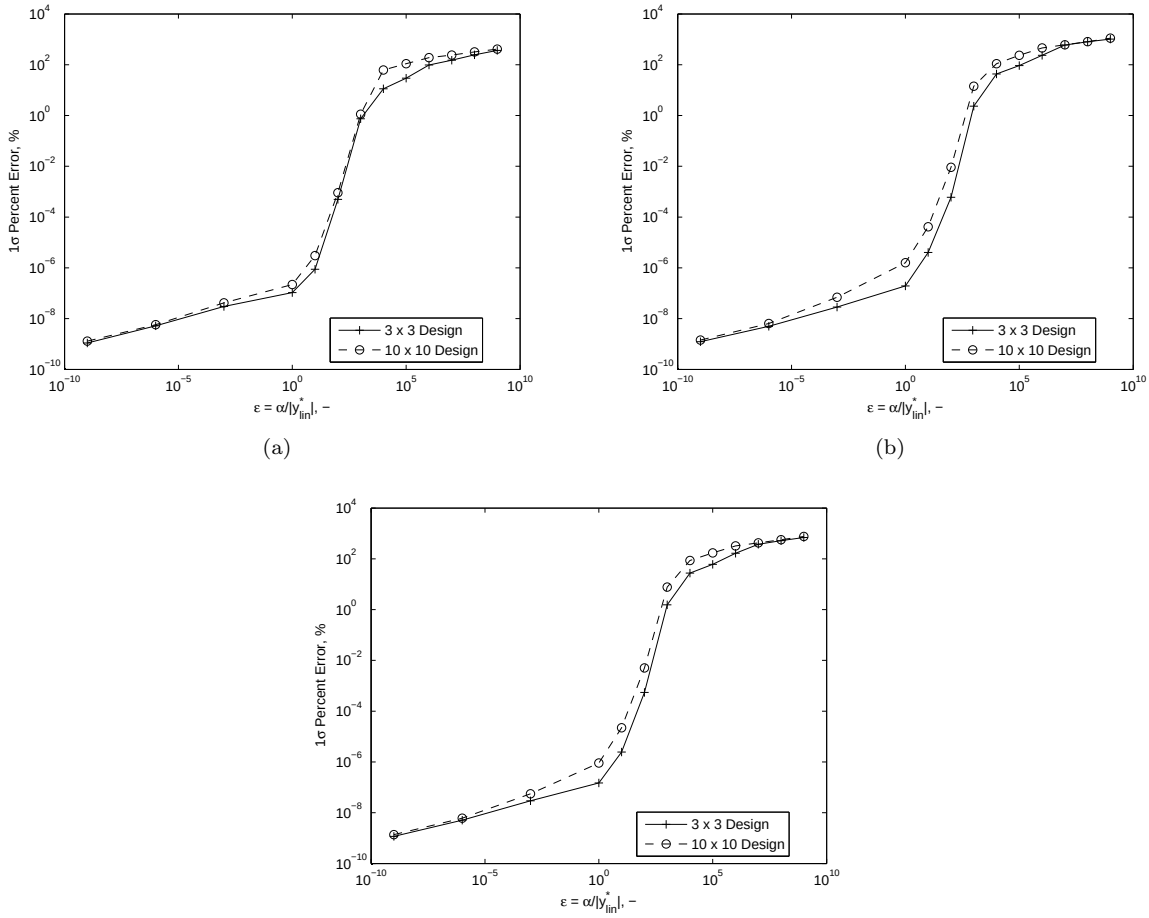

Figure 8. Variation in the computed accuracy of the rapid robust design methodology with the degree of nonlinearity. Three different nonlinear functions are shown, (a) $\sin(y)$**, (b)** $\ln(y)$**, and (c)** $(-1)^y$**.**

VII. Conclusions

The limitations and extensibility of the rapid robust design methodology from computational and accuracy perspectives were discussed. The effect of problem scaling on computational cost was considered two different ways. The first examined individual effects such as the number of design variables, nonlinearity of the CAs, and nonlinearity on the computational cost. The second considered computational cost through development of several potential complexity metrics. Relative to traditional robust design methods, the rapid robust design methodology developed scaled better with the size of the problem and had performance that exceeded the traditional techniques examined. In addition to computational cost, the accuracy of applying a method with linear fundamentals to nonlinear problems was examined through nonlinear perturbation analysis to identify the region of applicability for the method. For a wide variety of problems if the magnitude of nonlinearity is less than 1,000 times that of the nominal linear response, the error associated with applying successive linearization will result in 1σ errors in the response less than 10% compared to the full nonlinear error.

References

[1]Steinfeldt, B. A. and Braun, R. D., "Utilizing Dynamical Systems Concepts in Multidisciplinary Design," *AIAA 2012-5655*, Indianapolis, IN, Sept. 2012.

[2]Steinfeldt, B. A. and Braun, R. D., "Design Covergence Using Stability Concepts from Dynamical Systems Theory," *AIAA 2012-5657*, Indianapolis, IN, Sept. 2012.

[3]Steinfeldt, B. A. and Braun, R. D., "Leveraging Dynamical Systems Theory to Incorporate Design Constraints for

Multidisciplinary Design Problems," *AIAA 2013-1041*, Grapevine, TX, Jan. 2013.

[4]Steinfeldt, B. A. and Braun, R. D., "Rapid Robust Design of a Deployable System for Boost-Glide Vehicles," *AIAA 2013-0031*, Grapevine, TX, Jan. 2013.

[5]Geller, D. K., "Linear Covariance Techniques for Orbial Rendezvous Analysis and Autonomous Onboard Mission Planning," *Journal of Guidance, Control, and Dynamics*, Vol. 29, No. 6, 2006, pp. 1404–1414.

[6]Christensen, D. and Geller, D., "Terrain-Relative and Beacon-Relative Navigation for Lunar Powered Descent and Landing," *AAS 009-057*, Breckenridge, CO, Jan. 2009.

[7]Geller, D. K. and Christensen, D. P., "Linear Covariance Analysis for Powered Lunar Descent and Landing," *Journal of Spacecraft and Rockets*, Vol. 46, No. 6, 2009.

[8]Scheinverman, E. R., *Invitation to Dynamical Systems*, Prentice Hall, Upper Saddle River, NJ, 1995.

[9]Maimon, O. and Braha, D., "On The Complexity of the Design Synthesis Problem," *IEEE Transactions on Systems, Man, and Cybernetrics—Part A: Systems and Humans*, Vol. 26, Jan. 1996, pp. 142–151.

[10]Braha, D. and Maimon, O., "The Design Process: Properties, Paradigms, and Structure," *IEEE Transactions on Systems, Man, and Cybernetrics—Part A: Systems and Humans*, Vol. 27, March 1997, pp. 146–166.

[11]Braha, D. and Maimon, O., "The Measurement of a Design Structure and Functional Complexity," *IEEE Transactions on Systems, Man, and Cybernetrics—Part A: Systems and Humans*, Vol. 28, No. 4, July 1998, pp. 527–535.

[12]Braha, D. and Maimon, O., *A Mathematical Theory of Design: Foundations, Algorithms and Applications*, Kluewer Academic Publishers, New York, NY, 1998.

[13]Otero, R. E., *Problem Decomposition by Mutual Information and Force-Based Clustering*, Ph.D. thesis, Georgia Institute of Technology, Georgia, May 2012.

[14]Vallado, D. A., *Fundamentals of Astrodynamics and Applications*, Microcosm Press, El Segundo, CA, 2001.

[15]Khalil, H. K., *Nonlinear Systems, 3rd Ed.*, Prentice Hall, 2002.